

REVIEW ARTICLE

Three-dimensional photonic bandgap materials: semiconductors for light*

C López

Instituto de Ciencia de Materiales de Madrid, Consejo Superior de Investigaciones Científicas (CSIC), and Unidad Asociada CSIC—Universidad de Vigo, C/Sor Juana Inés de la Cruz 3, 28049 Madrid, Spain

E-mail: cefe@icmm.csic.es

Received 10 June 2005, accepted for publication 22 March 2006

Published 20 April 2006

Online at stacks.iop.org/JOptA/8/R1

Abstract

Photonics, the technology of photons (by analogy to electronics, the technology of electrons) will be the driving force for the advancement of areas such as communications and computing, information technology and probably others such as sensing. Photonic band gap (PBG) materials may answer many of their demands. Trying to understand the physics involved is a challenge very eagerly taken on by an ample science community. Although most of the notions dealt with in this discipline are rooted in solid state physics concepts, it is worth pointing out that they were originally borrowed by solid state physics from the theory of electromagnetism. The realizations of actual structures to fulfil theoretical predictions are plenty and they come from very distinct fields. Foremost among the approaches to PBGs, colloidal systems lend themselves to being used as natural starting points for the purpose of creating and using photonic crystals. A broad range of techniques and different sources of knowledge contribute to the interdisciplinary nature of the subject. A whole wealth of materials properties are involved that spring from their architectural scale. From the molecular level, and up to the macroscopic structure, micro- and mesoscopic regimes involve new properties, processes, and phenomena like synthesis in new environments, mechanical, optical, electronic, magnetic and other properties.

Keywords: photonic band gap, opal, infiltration, templating, photonic crystal, diffraction, spectroscopy, fabrication techniques

(Some figures in this article are in colour only in the electronic version)

In this review a presentation of the concepts relating to photonic band gaps is made followed by a summary of the most successful realization strategies. Finally a review of the optical properties is accompanied by examples of applications directly derived from them.

* This article was submitted to the special issue on fundamental aspects of nanophotonics. This special issue may be accessed online at stacks.iop.org/JOptA/8/i=4.

1. Introduction

Photonic crystals (PCs) or PBG materials are a class of material structures in which the dielectric function undergoes a spatially periodic variation. The length scale in which the variation takes place (lattice parameter) determines the spectral range of functioning of the PC and the wavelength at which the effects are felt corresponds approximately to the lattice parameter. This can be achieved by structuring a single compound or by constructing a composite with materials of different dielectric

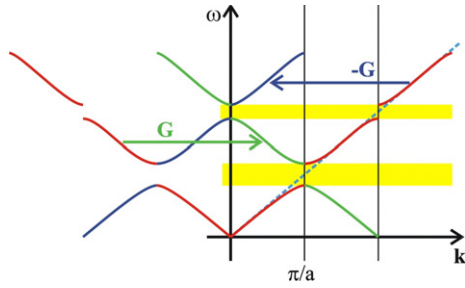


Figure 1. Dispersion relation for a homogeneous material (dashed cyan straight line) and for a periodic material with the same average RI and period a .

properties. Thus a PC working in the optical range of the electromagnetic spectrum will present a modulation of the dielectric function with a period of the order of one micron; one designed for microwaves should be modulated with a period of some centimetres; and a PC for x-rays should present a modulation of some ångströms and this is a solid state crystal. These present iridescences as a result of diffraction. Some natural examples are the multilayered structure of pearls, the flashing wings of several insects [1] and natural opals [2]. The same effect appears in familiar man-made objects such as compact discs or diffraction gratings.

When modelling the diffraction of light by periodic media, for example a layered structure, one computes the phase difference accumulated by rays that suffer scattering in different planes in the stack and adds up those with a multiple of 2π (constructive interference). With a little more algebra this leads to Bragg's law. A similar approach yields the (equivalent) Laue formulation and both lead to the concept of reciprocal lattice. This is a lattice (in a wavevector space) all of whose points generate plane waves with the periodicity of the direct lattice [3]. This simple formulation provides a description of the diffracting properties of the (periodic) system in the form of sets of pairs of the form [wavelength, direction] for which the light does not enter the structure but, rather, is Bragg diffracted. For any given direction several orders of diffraction may be considered, inspiring the idea of various bands for a given wavevector. This description is well suited to x-ray scattering for which it was developed. It relies on the fact that in these wavelength ranges the refractive index (RI) negligibly differs from one since the energy of the photons involved is immensely larger than the elementary excitations in the material and therefore there is no absorption.

A simple model for optical frequencies might be a one-dimensional (1D) periodic variation of the dielectric function. Fourier expansions of periodic magnitudes always become a summation rather than an integral. This summation contains a discrete (though infinite) number of plane wave-like terms, each corresponding (not by chance) to a vector of the reciprocal lattice. The dielectric function can then be expanded in such a way, and so can all other periodic magnitudes involved. If introduced in a scalar wave equation this leads to a dispersion relation: an expression for the wavevector as a function of energy. This is a band structure. The interesting result is that, for certain energy ranges—marked as stripes in figure 1—no purely real solutions exist and the wavevector has a non-vanishing imaginary part, meaning that the wave suffers

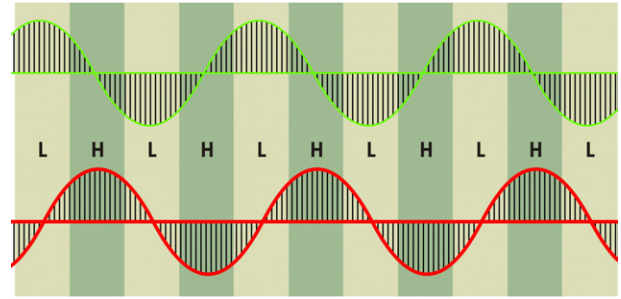


Figure 2. Two wavefunctions which have the same wavevectors and only differ in a phase have different energies because they take larger values in a layer of larger or smaller dielectric function.

attenuation and does not propagate through an infinite crystal. The wavevector at which this happens is that predicted by Bragg's law (producing stationary waves) and the range of energies where \mathbf{k} is no longer real is called the stop band. Another interesting fact is that for this wavevector there are two solutions (energies): one above and one below the gap, both having the same periodicity but spatially shifted with respect to each other. The electromagnetic (EM) energy is proportional to the dielectric function and the electric field squared, thus accounting for different energy despite both states having the same wavevector. An EM field stores more energy if it has extrema (rather than nodes) at the regions of higher dielectric function so that lower energy states concentrate in high dielectric function regions (see figure 2)¹. The stop band width is mainly determined by the dielectric contrast: the greater the contrast the wider the gap. It also explains that even infinite crystals will present a finite diffraction peak width as opposed to x-ray diffraction where peak width ($\Delta\lambda/\lambda \sim 10^{-6}$) is mainly accounted for by crystal size broadening (Scherrer's law). This very simple model can be further improved if we wish to consider the three dimensions [4]. If a single Fourier term in the expansion is assumed to dominate the sum close to a diffraction, simple expressions are obtained that fairly account for the width of diffraction peaks for common structures [5].

A rigorous treatment is required to account for all possible effects associated with the vectorial character of electromagnetic radiation. This can be done by expanding the electromagnetic fields in plane waves and solving the Maxwell equations exactly in a numerical fashion. This strategy was first demonstrated for periodic arrangements of spherical atoms in face-centred cubic (fcc) [6] and diamond lattices [7]. After a little manipulation, the Maxwell equations can be reduced to a wave equation of the form

$$\nabla \times \left[\frac{1}{\varepsilon(\mathbf{r})} \nabla \times \mathbf{H}(\mathbf{r}) \right] = \frac{\omega^2}{c^2} \mathbf{H}(\mathbf{r})$$

which is an eigenvalue problem for $\mathbf{H}(\mathbf{r})$, the magnetic field. It can be shown that the operator acting on the field ($\Theta = \nabla \times 1/\varepsilon(\mathbf{r})\nabla \times$) is Hermitian and, as a consequence, its eigenvalues are real and positive. That these are the properties of a Hamiltonian in quantum mechanics offers the possibility

¹ This can be otherwise viewed as a statement of a variational principle. The lowest energy eigenvalue is always orthogonal to all those of smaller energy and minimizes the energy functional $E_f = \frac{1}{2} \langle \mathbf{H}(\mathbf{r}) | \Theta | \mathbf{H}(\mathbf{r}) \rangle / \langle \mathbf{H}(\mathbf{r}) \cdot \mathbf{H}(\mathbf{r}) \rangle$.

to extrapolate many properties from quantum mechanics: we may think of PCs in solid state physics terms [8]. Since $\varepsilon(\mathbf{r})$ is periodic we can use Bloch's theorem; we also expand all fields in plane waves. After some more algebra this equation is reduced to a matrix diagonalization problem whose eigenvalues are the photonic bands, that is, lists of pairs of the kind $(\omega, \mathbf{k})_n$ that can be viewed as successions (labelled by n) of energies ω for every wavevector \mathbf{k} or series of functions $\omega_n(\mathbf{k})$. It is crucial to realize that, due to Bloch's theorem, two states with wavevectors differing by $2\pi/a$ represent exactly the same state. Therefore this wavevector \mathbf{k} can be confined to the first Brillouin zone (BZ): a region of reciprocal space closer to the origin than to any other reciprocal lattice point². If desired, the bands can be unfolded and extended in reciprocal space. This is schematically depicted for a 1D system in figure 1 where energy dispersion is folded back into the BZ by subtracting some reciprocal lattice vector. It should also be pointed out that the periodicity of the system changes wavevector conservation into conservation save for a reciprocal lattice vector \mathbf{G} . This acquires importance when analysing scattering processes where momentum must be conserved and, thus, incoming \mathbf{k}_{in} and outgoing \mathbf{k}_{out} momenta must satisfy $\mathbf{k}_{\text{out}} - \mathbf{k}_{\text{in}} = \mathbf{G}$. Eventually this may reduce to the ordinary $\mathbf{k}_{\text{out}} = \mathbf{k}_{\text{in}}$ for $\mathbf{G} = 0$.

This is acknowledged to be the correct description of photon states in a periodic medium. The conditions for gap appearance in these systems are much more restrictive than for electrons in solids. There is yet another subtle difference: for photons there is no length scale involved as a Bohr radius. This lack of an absolute length scale makes the physics of PCs scalable provided no dispersion of the dielectric function is assumed. In such circumstances resizing the system resizes the energy in such a way that the spectrum in units of c/a is independent of size, where c is the speed of light and a the lattice parameter. That is, if we scale a system such that the ratio of the wavelength to the lattice parameter stays constant all the properties of the initial system at the initial wavelength range are the same as those of the scaled system at the corresponding wavelength range. Since $\omega/(2\pi c/a) = a/\lambda$ it is customary to use such units to measure the energy. Besides the scalability in space there is a scalability in the dielectric function: there is no fundamental scale for ε . Two systems whose dielectric functions scale by a factor $\varepsilon'(\mathbf{r}) = \varepsilon(\mathbf{r})/s^2$ have spectra scaled by the same factor: $\omega' = s\omega$, which means that increasing the dielectric function by four decreases the energies by two.

Periodicity can be made to occur in one, two or three directions. Most of the properties discussed so far are independent of dimensionality and are well exemplified by sticking to one-dimensional systems. Such systems, extensively used in optical applications, are called Bragg reflectors and consist of stacks of alternating high and low RI transparent materials that base their superiority over metallic mirrors on their reflectance without dissipation. There are however certain aspects that might require some inspection when more dimensions are considered. Two-dimensional

² In order to obtain the BZ for any given reciprocal lattice it is sufficient to draw the bisectors (lines in 2D systems and planes in 3D) of the segments joining the origin with the lattices points and selecting the region that can be reached without crossing any such bisector.

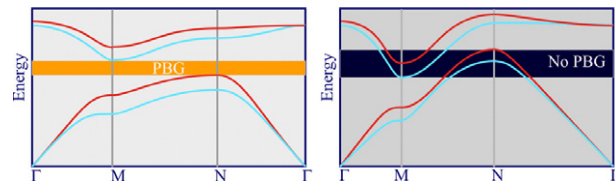


Figure 3. Two examples of two-dimensional PCs with different aspect ratios that cause the existence or absence of a full band gap. If the point N is much further than M from the origin its associated gap can have no overlap with that of M.

systems are increasingly used for microphotonic applications and consist of periodic repetitions of objects in a two-dimensional arrangement like, for instance, rods periodically arranged parallel to one another. In this case the dielectric function varies periodically in a plane perpendicular to the rods' axes but it is independent of position along the axis. Three-dimensional systems present a modulation in the third direction as in a stack of spheres. Since the energy spectrum is direction dependent a gap found in one direction will not be a real gap if there are states in other directions for this energy. This gives us an initial clue as to how to search for systems showing a full gap. If periodicity in one direction is very different from other the BZ will present a high aspect ratio (see figure 3). Close to the origin ($k \rightarrow 0$ or $\lambda \rightarrow \infty$) bands are straight lines since the system behaves as an effective medium with an effective RI for which $\omega = (c/n)k$. The gaps at the BZ edge can be expected around $\omega_{\text{BZE}} = ck_{\text{BZE}}/n$ with $k_{\text{BZE}} = \pi/a$ where a is the period in a given direction. If a takes very different values in different directions (for a multidimensional system) then gaps will open at very different frequencies and, consequently, will not overlap: no full gap will open.

2. The photonic band structure

Let us now turn to some aspects of the band structure that will help in interpreting optical spectra later on. For this, a good starting point is introductory solid state physics text books and specialized sources [9], but we shall summarize the most important results. A typical 3D dispersion diagram is shown in figure 4. The X axis represents momentum that for most purposes can be taken as representing wavenumber and direction of propagation. The Y axis represents energy measured in very convenient adimensional units: a/λ , where a is the lattice parameter. The different panels composing the diagram represent paths between important (high-symmetry) points in reciprocal space which (not by chance) happen to be the midpoints of the segments joining the origin to its nearest neighbours in the reciprocal lattice. Panels starting at Γ , e.g. ΓX , show the dispersion relation for states with increasing \mathbf{k} , all pointing in the same direction ($X = [001]$) whereas in panels such as XW both direction and modulus of \mathbf{k} vary continuously to sweep from the centre (X) to the corner (W) of the square faces of the fcc BZ. It can be seen that the panels have different widths according to the different distances in reciprocal space between the indicated (high-symmetry) points. Among the many bands that are plotted in the ΓL panel, some have the familiar $\omega = (c/n)k$ form

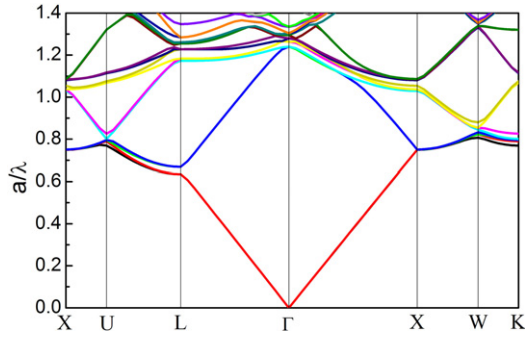


Figure 4. Dispersion relation for a PC made of silica spheres in a compact fcc arrangement. For these structures the lattice parameter is given by $a = D\sqrt{2}$ with D the sphere diameter. Owing to the scalability of the theory, the band diagram is independent of lattice parameter (and, thus, of sphere size) so long as the dielectric function is not dispersive. Therefore any such structure can be modelled by a single band diagram.

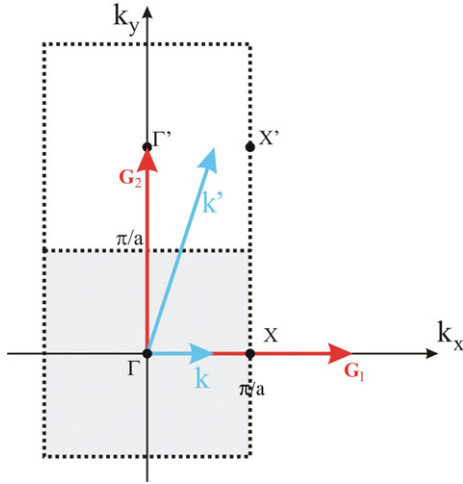


Figure 5. An arbitrary wavevector, \mathbf{k}' , is folded back into the first BZ, \mathbf{k} , by subtracting the closest reciprocal lattice vector (\mathbf{G}_2).

(n being an effective RI) or $\omega = (c/n)(k - 2\pi/a)$ which results from shifting the previous relation by one reciprocal lattice vector parallel to the vector involved. This is shown in figure 1 as a translation of the red curve by $2\pi/a$.³ There are other bands that result from the folding back into the BZ by means of vectors not parallel to the ΓX direction as depicted in figure 5. These bands have an expression like $\omega = (c/n)k' = (c/n)[(2\pi/a)^2 + k^2]^{1/2}$ which makes them less dispersive. This picture gets even more complicated for three dimensions, where many more vectors get involved, and is only simplified by symmetry properties making the bands degenerate. Of course this degeneracy may be lifted, for instance, by a slight deformation.

In figure 4 we can see that, in any given panel, not all energies have an associated \mathbf{k} . The regions where bands leave unfilled spaces are the gaps. By looking at the whole

³ It is worth noticing that the point X ([001] direction) does not show such a gap at the edge of the BZ, which is in agreement with a simple prediction based on the structure factor, as in x-ray scattering. However, if the dielectric contrast is strongly increased a small gap opens, signalling the failure of that theoretical approach.

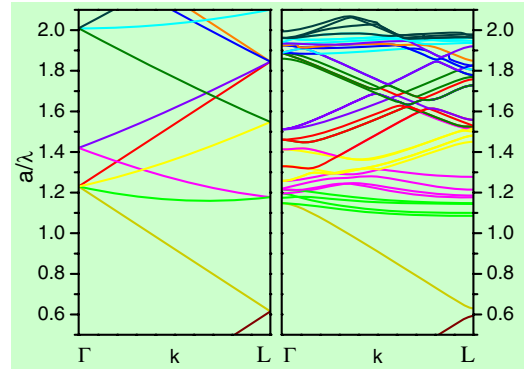


Figure 6. Comparison between no contrast and high contrast with the same structure. The bands in the right have been coloured, trying to convey the origin of the band in the homogeneous medium (left) but mixing of bands impedes it.

diagram we can see that none of these gaps is present for all wavevectors: there are no full gaps.

As mentioned before, RI contrast enhances the width of the gaps. If we continuously tune the contrast down to a homogeneous medium with the same average RI the bands evolve to a situation where no gaps are left; the bands cover the whole spectrum. This can be expressed by saying that larger Fourier coefficients lead to larger gaps and large Fourier coefficients are synonymous with strong modulation. An example is provided in figure 6, where two band structures are calculated⁴ that correspond to an fcc lattice of spheres in close packing. The left band structure corresponds to a lattice where the spheres have an RI very nearly identical to the background, whereas the right band structure corresponds to a system in which the background is air but the spheres have a high RI such the average is the same as in the left. There are several effects that can be seen. Firstly gaps open, for example in the edge of the BZ where the bands flatten. Secondly, bands curve and interact with one another, producing crossings and anticrossings, and generally flatten out as higher energies are considered. It can be seen that the energies of all the features are more or less the same in both cases. In the figure the bands are colour coded to point out their origin in the negligible contrast (*free photon*, in analogy with the solid state case) approximation and highlight the similarities. The gap widths are governed by refractive contrast while the gap positions are governed by the average RI. However, the existence of complete gaps very strongly depends also on the topology. The lattice alone does not determine the band structure: the shape of the *atoms* also plays an important role. As suggested above, the symmetry of the unit cell may lift degeneracies that, eventually, can open gaps. That is the reason why so many more bands show up in the finite contrast band structure as compared to the homogeneous medium.

In summary the best chances to find a structure with a complete gap are for lattices with as round as possible a BZ, with a primitive cell with non-spherical atoms inside and with the highest possible RI. In three dimensions this points towards the fcc lattice [11], a particular case of which is the diamond

⁴ Photonic band structures are computed using a plane wave basis in an iterative implementation as described in [10].

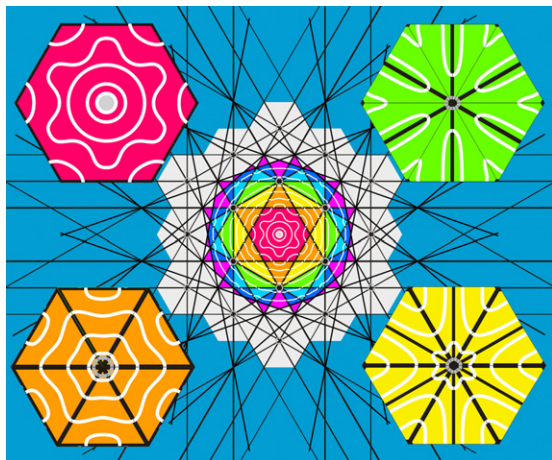


Figure 7. Construction of IFSs in a hexagonal lattice. Initially the IFSs can be drawn as circles that bend upon crossing Bragg planes in order to meet them perpendicularly. By translating the curves into the first BZ by the appropriate lattice vectors it is possible to build the different IFSs corresponding to higher and higher energies.

lattice where every lattice site contains two atoms. It can also be shown that very low filling fraction (the portion of space filled by the scattering material) is desirable.

An additional aspect that brings about very important consequences and gives rise to applications is the deformation of the isofrequency surfaces (IFSs)⁵. This is caused by the fact that an IFS must cross Bragg planes (boundaries between reciprocal lattice unit cells) at right angles to them [12]. This can only be achieved if the IFSs are bent and warped in the neighbourhood of such planes, as is schematically depicted in figure 7. Here the reciprocal space of a hexagonal 2D crystal is represented. The centre point is the origin and the light grey hexagons represent repeated BZs that tile the whole space each surrounding a lattice point. The coloured polygons are fractions of BZ bounded by Bragg planes (bisectors of the segments joining lattice points). Every successive BZ is divided into more and more fractions: the first one (red, centre hexagon) is one piece (see top left inset); the second (orange) is divided into six pieces (bottom left inset); the third one (yellow) is divided into twelve (bottom right inset), and so on. These pieces can be brought to form a BZ in the origin by translating them by the appropriate reciprocal lattice vectors. For low contrast the IFS are circles but the introduction of contrast obliges to break them into curves whenever a Bragg plane is crossed. When the m th BZ is recomposed from its fragments bringing the IFS sections it contains to the origin, successive IFSs are built, as illustrated by the coloured hexagons in the corners of figure 7. These IFSs become useful when exploiting the superefractive properties of PCs. When bands depart from the *free photon* behaviour ($\omega = ck/n$) the RI must be taken as $n = c/(d\omega/dk)$ rather than $n = c/(\omega/k)$ and very peculiar behaviours can be obtained. The group (or energy transmission) velocity, the only meaningful one in these systems, is now $v_g = d\omega/dk$ rather than $v = \omega/k$. Near the centre and edges of the BZ the bands flatten out and the group

⁵ Of course only for homogeneous media, low RI contrast (free photon approximation) or long wavelengths are these IFSs spheres of radius $k = \omega n/c$.

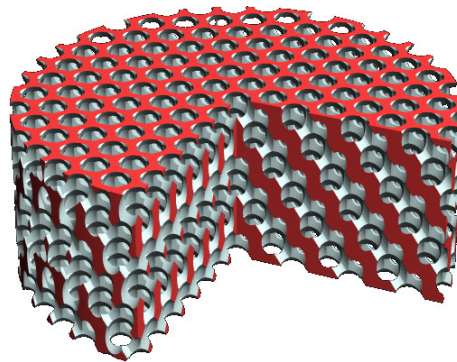


Figure 8. Yablonovite: the first 3D structure built to have a complete PBG.

velocities go to zero. The net effect is that the time taken by the EM field to traverse the sample is dramatically increased, enhancing the interaction between light and matter. Since, for multidimensional systems, the derivative is actually a gradient, the correct expression for the velocity in the n th band is

$$\mathbf{v}_n(\mathbf{k}) = \nabla_{\mathbf{k}} \omega_n(\mathbf{k})$$

which means that propagation is (as the gradient) normal to the IFS concerned. For energies near or beyond the first BZ the IFSs cross many Bragg planes and are strongly distorted. We can visualize this by taking horizontal sections in figure 4 and seeing that different \mathbf{k} are required to cross a band if searching in different directions. This has important consequences because, in this situation, the propagation direction may greatly differ from the wavevector. If the energy is changed the surface also changes shape, with the corresponding change in propagation direction. At some points this change may be rapid, with the associated swing in direction for small changes in energy, and the system may be used to separate very similar frequencies.

3. Top-down fabrication methods

The fabrication of PCs has evolved dramatically since they were first proposed [13]. The first realization of a complete PBG crystal was performed by Yablonovitch after a feverish search of materials and structures [14]. This was machined into a low loss dielectric material with millimetre-size drills. The size determined its working range to be in the microwave regime. The way it was obtained was by boring three tilted holes in each position of a hexagonal lattice marked on the surface of the block of material. The network of holes excavated the material and left behind a structure similar to a silicon lattice (see figure 8). It was tested and shown to reject radiation of certain wavelength in any direction it entered the material.

The race was then started in pursuit of ever smaller scales in order to reach the optical regions where most applications were designed. Different dimensionalities were attempted depending on the application in mind and, in some respects, it is difficult to assign a dimensionality to some such structures. They are sometimes described according to the number of dimensions in which the PC effect is felt and sometimes according to the opposite criterion. Thus

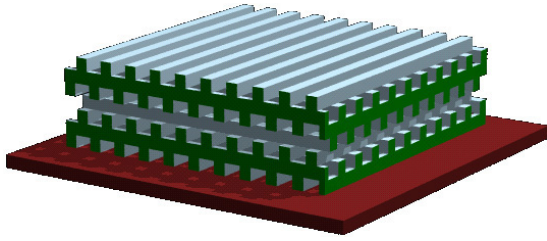


Figure 9. Wood pile structure built in a layer by layer fashion using lithography.

2D systems like multilayers are effectively 1D PCs. They have been widely produced and used for a long time as, for instance, antireflection coatings, notch filters or distributed Bragg reflectors. Usually evaporation techniques are used.

The fabrication of planar systems, where the PBG is felt in two dimensions, has experienced the greatest development by using mature techniques borrowed from many areas. Lithography (optical and electronic) is the main contributor to this expansion based on the microelectronics thirst for increasingly precise processing. These 2D PC structures have acquired the widest diffusion due to the easy, albeit expensive, implementation of microelectronic technology techniques such as photolithography and electron beam lithography. Monorail and air bridges are examples of 1D structures also produced by these means [15].

Typically Si and III–V semiconductor technology is applied. Lattices composed of holes or pillars were often adopted to obtain different structures. The first such realization was in GaAs/GaAlAs [16] where a lattice of holes was etched through an e-beam lithographed mask. Wave guides (WGs) can be defined in these structures by leaving rows of holes filled. Point defects produced near such multiple wavelength carrying WGs can be tuned for extraction of selected wavelengths [17]. Although these techniques are mostly applied to produce 2D systems (where they are most effective) they can also be used in conjunction with other processes to add a third dimension to the structures obtained. By using relatively standard microelectronics techniques in a layer by layer fashion, 3D crystals were soon fabricated for the IR region [18]. The process consisted in lithographically defining a 2D array of bars in a thin layer of Si, the empty space among which is subsequently backfilled with silica and planarized. A second layer of Si is deposited and the processing repeated, drawing the bars at right angles to the first set. These are backfilled and planarized and the process started over again. Finally all the silica is etched away and a 3D porous structure like that presented in figure 9 is obtained. Care must be taken to place the bars such that the nearest parallel sets do not overlap vertically. As an alternative, wafer bonding was used to build the same 3D structures in which WGs can be easily integrated during production [19]. In figure 10 an example of another fabrication approach is shown [20]. The process here consists in making a pattern of vertical holes in a hexagonal arrangement in an amorphous Si layer and backfilling it with spin-on dielectric. The latter is etched and polished to the level of the underlying Si and subjected to a second Si growth, lithographic recording and etching process taking care that the new set of holes' positions and depths are such that the layer

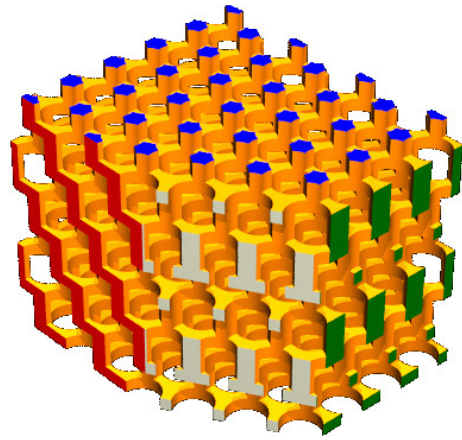


Figure 10. 3D structure obtained with a layer by layer method in which successive etching/backfilling processes are carried out using photolithographic techniques.

underneath is partially perforated with a sequence similar to that of an fcc lattice in the [111] direction. Those regions where holes belonging to different cycles overlap present a columnar configuration because groups of six holes leave little material untouched. If the cycle is repeated and finally the backfilled dielectric is dissolved, a stack of layers of columns and layers of holes is obtained that mimic the bonds in a diamond lattice. This method presents the advantage that four lithographic processes yield seven lattice layers.

Methods capable of producing entire regions of PBG material were developed based on holographic techniques in which several beams are made to interfere in the presence of a photosensitive resist that is polymerized to fix the pattern and create a replica of the intensity above a certain threshold. This is schematically shown in figure 11, where examples are given of various dimensionalities. When two coherent plane wave beams interfere, equal phase regions are planes whose normal vector is the difference in wavevector between the two interfering beams. Thus, the threshold for photopolymerization defines a boundary that coincides with a given intensity and correspondingly to a phase difference. The net results will be parallel slabs of polymerized and non-polymerized monomer alternated in the direction of the wavevector difference. When three beams are made to interfere, two wavevector differences can be defined that produce two such interference patterns. The net result is two 'crossed' sets of parallel slabs that give rise to a 2D pattern. If four non-collinear beams are considered a 3D pattern is created. The period of the structure and its symmetry (lattice) are dictated by the laser wavelength, the relative phases, and incidence directions of the interfering beams, whereas the shape of the repeated feature in the lattice (basis) results from the beams' polarizations [21]. Exposed but undeveloped films are amenable to further processing by laser scanning to draw new structures for WG fabrication [22]. Simplified versions of this technique are being developed where not four but two laser beams are made to interfere. The interference of two beams yields a one-dimensional stack of layers, but if this process is repeated, after the polymer film is rotated, a 3D lattice can be created [23]. This greatly simplifies the method because the experimental set-up involves many fewer parameters while the time remains more or less the same.

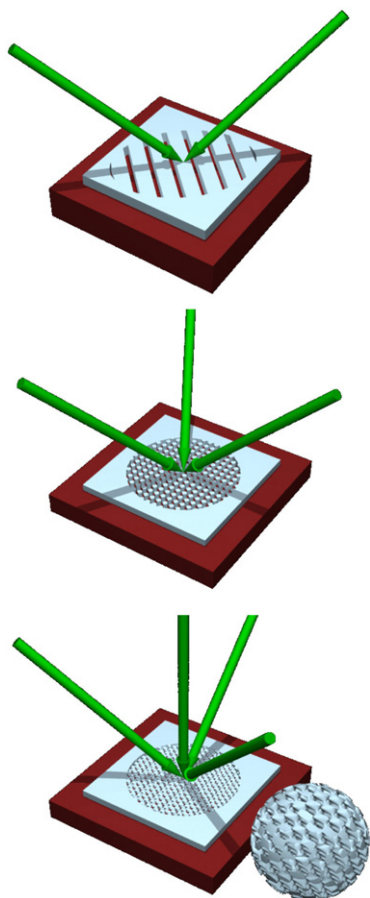


Figure 11. Holographic interference permits the use of different configurations to produce PBG structures of any dimensionality by interference of the appropriate laser beams. One-, two- and three-dimensional examples are provided. The spherical shape in the bottom example is a magnified view of the structure obtained.

These methods have opened the field to new ones where the photosensitive polymer is scanned with a CW laser rather than exposed with a laser shot. This is called direct laser writing and although it is a much slower method it has the advantage that it can produce any structure, be it periodic or not, meaning that defects can be integrated at the time of writing. Layer by layer structures can thus be fabricated. Femtosecond laser pulses are tightly focused inside the liquid resin, which is transparent to pulses below the two-photon absorption threshold power density. The pulse intensity is adjusted so that the light power density at the focal spot of the laser beam exceeds the threshold. Strong absorption in this highly spatially localized region results in photopolymerization of the resin. By scanning the coordinates of the focal spot, pre-designed patterns can be recorded in the liquid resin. Laser irradiation renders the exposed regions insoluble, while unexposed regions are dissolved and removed during the post-processing stages [24]. Using these same methods interesting topologies have been written [25], imitating previous attempts [26] to grow spiral structures that hold great promise for practical applications [27] and the highly appreciated wood pile structure [28].

Robot manipulation is a recently developed method that allows the arrangement of nano- and microscopic objects with

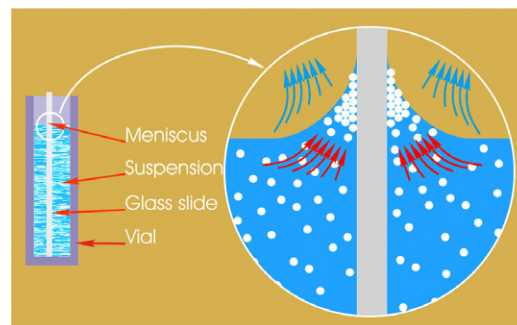


Figure 12. Vertical sedimentation method. A flat substrate is immersed in a vial containing the colloid and the solvent is allowed to evaporate.

a precision of nanometres, and has allowed the assembly of diamond opals [29]. The wood pile structure, that has revealed itself as one of the best suited to sustain a complete PBG, is amenable to construction by this method. Recently this has been demonstrated by stacking grids with the use of a nanorobot [30]. The grids were previously fabricated by lithography as wires held by a frame and they were stacked criss-crossed to form a 3D crystal. Crystals for infrared wavelengths of 3–4.5 μm of four to twenty layers (five periods) including one with a controlled defect were integrated at predefined positions marked on a chip with accuracy better than 50 nm. Microspheres are used to slot into holes defined in the frames to ensure correct alignment.

4. Self-assembly methods

Artificial opals have gained a position as photonic crystals (PCs) as inexpensive alternatives to other more sophisticated PC fabrication approaches. Methods for opal preparation are usually based on the natural tendency of microscopic colloidal particles of silica, polystyrene (PS) or polymethylmetacrylate (PMMA) to self-assemble in an ordered face-centred cubic (fcc) structure. However, the main problem found in the preparation of artificial opals is the unavoidable presence of some sort of disorder generated by both the polydispersity of the microspheres used and the inherent stacking defects developed during the growing process. Many efforts have been devoted to improve the quality of the opaline samples in the last few years, by using different methods of preparation, such as sedimentation [31], electrophoresis [32], confinement in special cells [33], vertical deposition [34] or some others introducing small modifications of these methods [35, 36].

The most widely used assembly method, vertical sedimentation, basically consists in submerging a flat substrate (e.g. glass or silicon) in a diluted colloidal suspension and allowing the solvent to evaporate (see figure 12). The meniscus that forms in the contact line between air, liquid and substrate sweeps down the substrate and deposits the spheres in a crystalline arrangement. Alternatively, spinning techniques can be applied for rapid fabrication of moderate quality but in large scale [37]. In this case a substrate is set to rotate at a controlled velocity and a controlled amount of colloid is dropped and allowed to spread. The concentration and spinning velocity allow one to determine the thickness of the

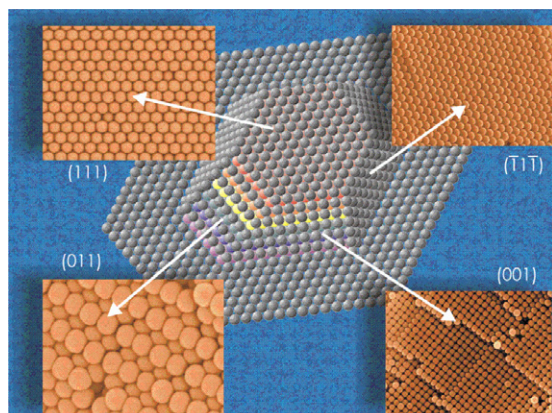


Figure 13. Crystal structure model of an artificial opal. The different facets shown are exemplified with actual SEM images from real samples.

resulting opals. The resulting crystal structures are fcc close-packed arrangements, as shown in figure 13.

These optical systems are ideal references for studying the intrinsic properties of a PC, such as the density of states inside the crystal [38] and gap formation [39], or to confirm theoretical predictions. An additional advantage is that their optical properties can be modified continuously in a controlled way, allowing the preparation of more sophisticated systems. One of the most usual methods is void infiltration with different materials. If a high RI material is used in the infiltration, the PC obtained may exhibit full photonic band gaps (PBGs) in the near infrared and visible range [40].

Semiconductors of such technological impact as silicon and germanium can be synthesized by chemical vapour deposition (CVD) [41, 42]. Here the sample is placed in a cell where the precursor gas is condensed with liquid nitrogen. Disilane (Si_2H_6) and germane (GeH_4) can be used as precursors for Si and Ge, respectively. Once the precursor gas is condensed, the cell is isolated and placed in a furnace at the selected decomposition temperature. Under these conditions both semiconductors grow amorphously and they can be crystallized by a later annealing. Two parameters govern the growth of the semiconductor: the precursor gas pressure and the reaction temperature. Decomposition temperature plays a very important role in two aspects: growth velocity and the presence of undesired particles. It has also been observed that high temperatures induce the growth of undesired particles. In the case of Si the precursor gas decomposition temperature selected was 375°C while for Ge it was set at 270°C . Lower temperatures result in very slow synthesis rates while higher ones allowed little degree of control. The growth takes place conformally (by creating a nanometre thin layer of material that covers all the surfaces of the template) and the result is a composite that can be further processed. In particular, the initial backbone can be removed, leading to what has been dubbed inverse opals, an example of which is depicted in figure 14.

The power of this method is that it allows not only growing these and other materials on silica but either on the other [43]. A further degree of freedom will be provided by the selectivity of different solvents that can be used to remove some of the materials.

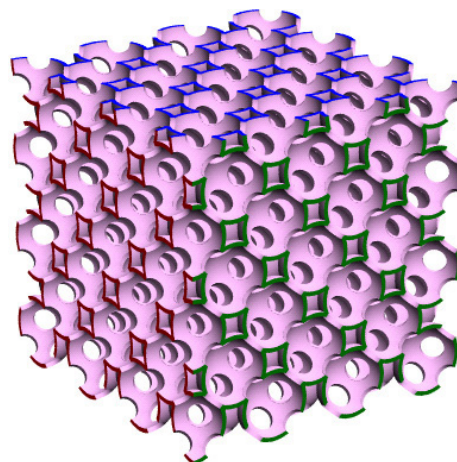


Figure 14. Typical aspect of an inverse opal where cleaved edges show (100) facets. Windows connecting the templating spheres can be clearly seen.

Recent work has shown that ‘band engineering’ can be achieved by multilayer infiltration with different materials or by obtaining new inverse structures through morphological changes of the material filling the voids [44]. Silica and PS spheres containing metallic or magnetic cores can be prepared [45, 46] allowing one to couple the metallic and/or magnetic properties, respectively, with the photonic ones. Using patterned surfaces as substrates, the fabrication of prisms [47] and microfibres [48] made of PC has been possible. Another possibility is the introduction of controlled defects in colloidal crystals by the use of two-photon polymerization [22] or laser micro-annealing [49]. By combining spheres of two different sizes, ordered superlattices [50] or structures containing planar defects [51] have recently been obtained.

5. Optical properties and applications

The optical properties of PCs are entirely determined and can be fully accounted for by their photonic band structure. In practical terms the bands can be used to interpret and predict the optical properties by using a few simple rules. Light coming from outside a PC will in principle travel through the PC if there are states belonging to the PC that preserve the energy and (parallel) momentum. The difference from ordinary dielectrics is that now not all energies are allowed to propagate through the crystal but only those that belong to a photonic band, meaning that light whose energy lies in photonic gaps will be reflected by the PC. This was in the core of the initial proposal of the concept of PC by Yablonvitch [52]. The refraction in the boundaries of the PC is also entirely determined by the band structure, but now momentum conservation takes on a new form to include the periodicity of the crystal. Thus the (parallel) wavevector of the incoming and refracted beams must differ by a reciprocal lattice vector that may or may not happen to be zero. When it is not we usually talk of diffraction rather than refraction, but we must bear in mind that the process involved is fundamentally the same. This gives us a hint that all processes in a PC and, in particular, the build up of a band structure, can be viewed as (coherent) multiple scattering.

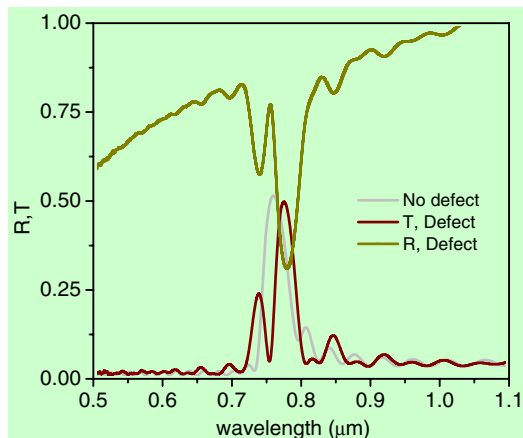


Figure 15. Typical reflectance (grey) of a finite PC (an opal in this case) and transmittance (brown) and reflectance (green) when a defect is inserted in the middle of such structure. Transmittance and reflectance are easily recognized for having a minimum and a maximum, respectively, in the energy of the gap.

Let us first analyse reflectance and transmittance. These are the easiest processes. By looking at the band structure (e.g. figure 6) we see that for the low energies the PC behaves simply as a homogeneous medium with an RI given by the slope of the first photonic band which can be estimated by taking the average of the composing materials weighted by filling fraction (relative volume of each component). Therefore, for the energies spanned by this band, transmission is mediated by its photonic states. In these circumstances all the light is transmitted and the reflectance is zero (see figure 15).

Since for low energies (long wavelengths) the medium is homogeneous and isotropic, IFSs are just spheres, refraction happens as in ordinary dielectrics and Snell's law is derived from (parallel) momentum conservation. As the edge of the BZ is approached the IFSs start to distort because the smaller slope of the bands requires larger wavevector increments to achieve the same increments in energy. Thus, lobes start to develop and the initially spherical IFSs become warped and twisted and are called *monsters*. In these circumstances refraction is anomalous in the sense that Snell's law may be viewed to happen with a negative RI (see figure 16). The superprism effect [53], all-angle negative refraction [54], high group velocity dispersion [55] or the improvement of nonlinear optics effects are all applications derived from the physics happening when bands are distorted (basically) by the proximity of Bragg planes.

When finally the edge of the BZ is reached the band splits and a gap is formed where no states exist; therefore light impinging on the crystal is reflected and the transmission drops to zero: standing waves form the gap edges and a Bragg peak appears in the reflectance spectrum (see figure 15).

The occurrence of the gap can also be viewed as the fulfilment of the Bragg law condition that can be stated as $\mathbf{k}_{\text{out}} = \mathbf{k}_{\text{in}} - \mathbf{G}$ or, in other words, the tip of the wavevector \mathbf{k}_{in} (and \mathbf{k}_{out}) lies on the Bragg plane associated with the reciprocal lattice vector \mathbf{G} [12]. Bearing this in mind it is easy to foresee that if the direction of incident light is changed the wavevector at which the gap will open will also change (the BZ cannot

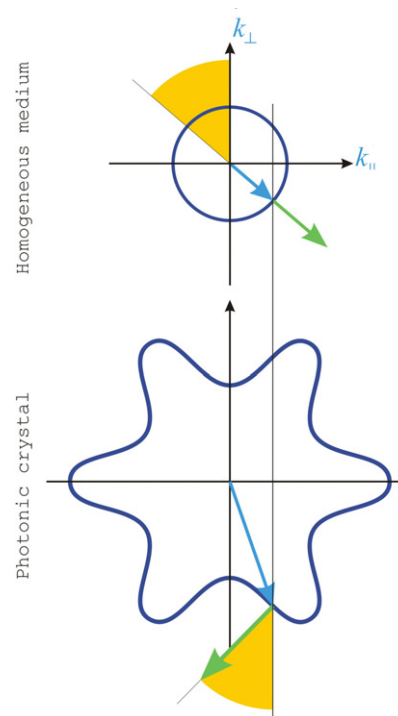


Figure 16. In homogeneous media, IFSs are spherical, $\omega = c|\mathbf{k}|/n$, and the propagation direction (green, arrow from the IFS) and wavevector (blue, arrow pointing from the origin to the IFS) are collinear. But in PCs these surfaces may become very anisotropic. Conservation of the parallel component of the wavevector leads to very peculiar refraction effects since the propagation is no longer collinear with the wavevector.

be round) and so will (in principle) the gap spectral position. The relationship between the wavelength and incidence angle is known as Bragg's law.

This, for a bare opal, is depicted in figure 17: a summary of spectral positions as the incidence angle (or the parallel momentum) is changed by tilting the incoming beam towards non-equivalent directions on the surface. This is done by rotating the sample around two perpendicular axes contained in the sample surface [56]. Here we can appreciate how the position of the Bragg peak (experimental data) follows the gap between the third and fourth bands which, for this system, bound the first gap. The two panels represent tilting in the two main directions: from L towards W and towards U (or K which is equivalent). Experimental results shown in the right panel present an avoided crossing behaviour [57, 58] taking place at the W point in reciprocal space where the incident wavevector fulfils simultaneously the Bragg condition for the $\{111\}$, $\{11\bar{1}\}$ and $\{200\}$ families of planes, and strong mode coupling takes place. If the centre frequency of these peaks is compared with calculated bands (see figure 17) a good agreement is found. Similar experiments (left panel in figure 17) carried out when the rotation axis is parallel to the growth direction may be compared with calculated bands along the Γ LU direction as would be expected due to the three-fold symmetry of the hexagonal facet of the BZ.

The occurrence of this gap can be taken advantage of in order to develop applications based in the (structural) colour of PCs. Thus infiltration of colloidal crystals with polymers

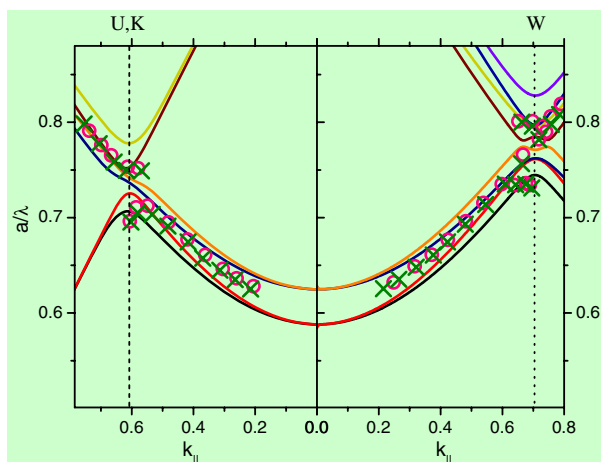


Figure 17. Experimental reflectance peaks (obtained at two sample positions separated by a rotation of 60° with respect to its normal) and theoretical (lines) bands when scanning the Γ LW region in reciprocal space. Knots and crosses represent data obtained by rotating the sample by 60° through its normal.

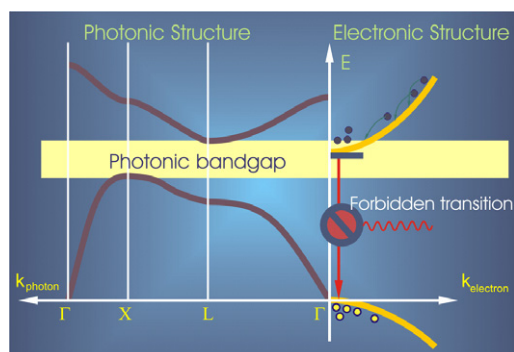


Figure 18. This diagram presents a simplified outline of the coupling between photonic and electronic band structure for the inhibition of spontaneous emission and laser action. Band to band recombination (provided by the electronic part of the device) is prevented because a photonic band gap at that energy is provided by the PC part. A defect state in the gap might open a channel for recombination.

or other organic compounds is a suitable method for the fabrication of photonic inks [59] or sensors [60], for instance. But the most sought for evidence in the field was spontaneous emission inhibition, and this was only recently found both in two dimensions [61] and three dimensions [62] by measuring photoluminescence emission rates in the presence/absence of a PBG. This phenomenon relies on matching the energy of the emission to that of a photonic band gap so that the emitted energy corresponds to a forbidden state. This is schematically depicted in figure 18.

The breaking of the crystal translation symmetry produces defects that place states in these gaps. These states, unlike the crystal ones, are not extended (propagating) but localized, and they can be regarded as the result of confinement of electromagnetic radiation by the PC at non-propagating energies. This localization of the EM field by defects in a photonic superlattice was at the heart of the initial proposal of the PBG from the point of view of the localization of light [63]. A simple example of such features is presented in figure 15 where a planar defect is introduced in an opal giving rise to

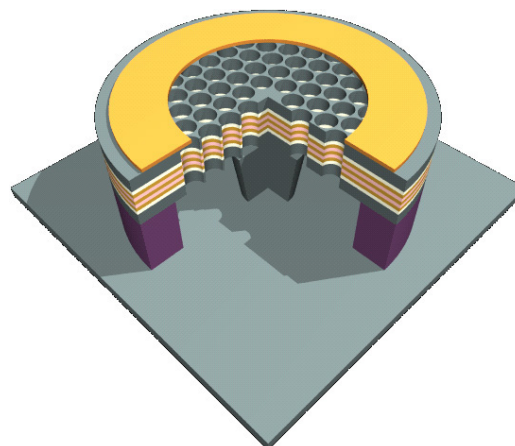


Figure 19. Diagram of a multi-quantum well electrically pumped laser. This laser is based on a 2D PC lithographically etched into a multi-quantum well where one or various holes are left undone to create a cavity in which the EM field is localized.

a minimum in reflectance (or a maximum in transmittance) in the centre of the Bragg's peak.

A point defect in the middle of the crystal can be viewed as a cavity where EM energy is stored. This very concept was exploited when 2D systems with a defect in the centre were stretched in the third direction to build fibres called photonic crystal fibres in which the defect constitutes the core through which the light travels and the surrounding PC constitutes the cladding [64].

If the cavity is near enough the boundary of the PC it may be charged and discharged by pumping light from the exterior. The inverse of the rate at which such cavity 'leaks' its energy is known as the quality factor, and it can be regarded as the number of oscillations a harmonic EM field suffers before escaping the cavity and, spectroscopically, it can be described as the ratio centre-to-width of the associated spectral feature.

This is a means to store energy and to guide it along paths drawn in the PC by a series of defects. The former can lead to the concept of a PC laser [65] whereas the latter is being extensively used for waveguiding. Typically a PBG laser is based on the coupling of an electronic part (capable of producing light through recombination of electron-hole pairs) with a photonic one (capable of inhibiting the spontaneous emission through a PBG). If a channel is provided for emission it is possible to balance gain and losses to produce amplification and laser action. Usually 2D PCs are employed, with confinement in the vertical direction being provided by total internal reflection and a single or a few missing holes acting as the defect concentrating energy. Optical pumping was initially employed but electrical pumping is also possible and has already been realized [66]. Of course, in this case a full PBG is employed since otherwise recombination could proceed by emission along directions not blocked by the partial gap. A model of such a structure is depicted in figure 19 where a multi-quantum well is lithographically drilled in periodic fashion to define a 2D PC in which a hole or a few holes are left filled to define a cavity. This cavity acts as a lasing centre in which the EM field is enhanced by virtue of the PBG.

If multiple point defects are chained together a coupling between their associated states may occur as molecular orbitals

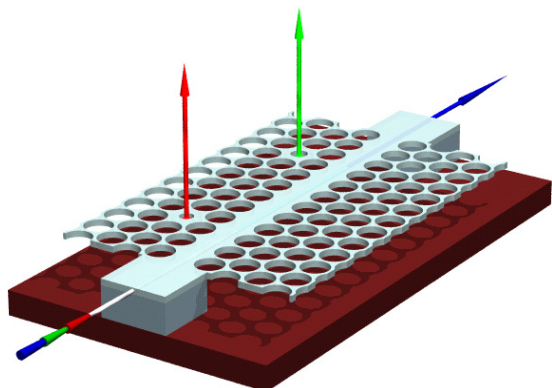


Figure 20. A drop filter can be implemented by placing designed defects near a waveguide such that only resonant light can be coupled out of the guide and extracted. This can be done by tuning the size of the defect.

are built from atomic orbitals. This of course leads to a band of states within the PBG than can serve to channel light through a PC. An example is provided in figure 20, where a drop filter is implemented based on this principle. Here a waveguide (one missing row of holes) couples to smaller (or larger) holes which act as defects that trap light and extract it out of the system [17].

We have so far accounted for the optical behaviour up to the energy of the first pseudogap in our model system: opals. If energy is further increased beyond the high-energy side of this gap, transmission resets in approaching unity again, and the reflectivity drops to zero because incoming light couples to the third and fourth bands. In actual finite systems this is not exactly true because reflection on the ends of the crystal build up Fabry–Perot oscillations that appear as evenly spaced ripples in the actual spectra (see figure 15). When the crystal is very thick (several tens of layers) the ripples disappear and only the peak is visible.

While the optical response of these opal-based PC is well known and easily understood in the low-frequency region where first-order Bragg diffraction (produced by the {111} family of planes) takes place, for higher frequencies the situation becomes more complex. The appearance of bands arising from wavevectors originally not parallel to the ΓL direction, but folded back into the first Brillouin zone by translational symmetry (recall figures 5 and 6), not only fills what would be a ‘second-order’ L gap with states but introduces anticrossings between bands of the same symmetry [9]. Higher-order Bragg diffractions by the {111} planes are also expected. This complicates the band structure, making the comparison between experimental spectra and calculated bands non-trivial. The above can be appreciated in figure 21, where transmission and reflection spectra at normal incidence are plotted together with the calculated band structure. Firstly we must notice that now, at variance with the previous case, the reflectivity (transmittance) never reaches values close to unity (zero) because many scattering processes are involved that carry energy away that never reaches the detector. This is related to the fact that higher-order diffractions are not associated with gaps as was the case in the first order, because bands are folded back that fill that gap. Nevertheless, most features in the reflectance spectrum find correspondence in the transmittance one.

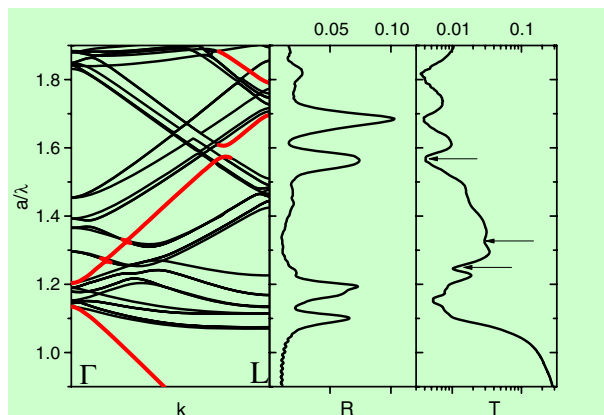


Figure 21. Band structure calculated along the ΓL direction in reciprocal space for an artificial opal. Reflection (centre panel) and transmission (right panel) measured at normal incidence can be compared with the bands. The arrows point at the peaks originating in anticrossings.

It can be observed that reflection peaks/transmission dips may be associated with perturbations (such as gaps and avoided crossings) found in those bands reminiscent of the free photon behaviour for wavevectors parallel to the ΓL direction⁶. For regions where these perturbations are absent, the crystal presents a low reflectance and high transmittance. This represents a first approach to the understanding of the optical properties of photonic crystals in this utterly interesting, though not yet fully explored, spectral region [67]. Finally, we must take into account the fact that light is being scattered out of the normal direction, as is evidenced by the optical diffraction results presented below. Due to the geometry of the experiment, this light will not be detected, and will certainly affect the experimental spectra. By examining the correlation between reflectance and transmittance with the bands it can be seen that some features correspond to gaps open in the bands, some to diffractions out of the direction of the detector, and some to anticrossings in the bands (marked with arrows in figure 21).

PCs are, by definition, periodic; therefore their Fourier transforms must be also periodic. The diffraction pattern can be regarded as the Fourier transform of the periodic array present in the PC, so that diffraction can be used to obtain reciprocal lattice of a given structure as has been done for years in x-ray diffraction techniques. This allows one, in particular, to orientate the crystal for probing the optical properties of the crystal along high-symmetry directions in angle resolved experiments.

Diffraction, however, can only be seen as one more expression of the interaction of external light with the PBG structure of the crystal and it can be fully accounted for by it [68]. In particular the onset of diffraction is clearly given by the appearance of the first band not corresponding to forward/backward propagation. This is a typical case where a band is folded back with a non-collinear reciprocal lattice

⁶ Small discrepancies can be attributed to the fact that the calculation of the bands was made assuming that the dielectric function is constant, which may prove a wrong assumption. But the most widely used and public access package, MPB, developed at MIT, only allows the use of constant dielectric functions.

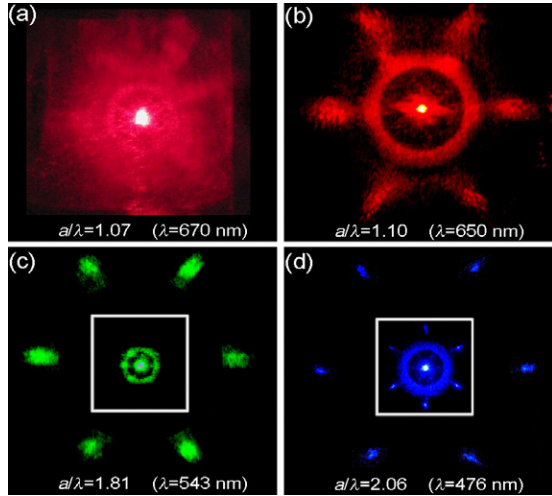


Figure 22. Diffraction patterns generated by opals made of (a), (b) 505 nm and (c), (d) 695 nm PS microspheres. The first two pictures are taken on the sample while the latter include both the sample (inset) and the diffraction pattern projected on a screen. Notice that the diffraction pattern shown in the sample in (d) is rotated 30° respect to the spots projected on the screen.

vector and that is the reason why it is not linear: ω does not tend to zero as the (reduced) wavevector \mathbf{k} tends to Γ . In fact the analysis in figure 6 indicates that the green band in the left panel originates from the dispersion relation $\omega = ck'$ with \mathbf{k}' such that $\mathbf{k} = \mathbf{k}' - \mathbf{G}_{(100)}$ lies in the first BZ and in the direction ΓL (that spanned in the panel). We see that, in addition to producing a feature in reflectance, it marks the beginning of a drop in transmission (see figure 21) just because light in transmission experiments fails to reach the detector as it is being diffracted elsewhere. This is shown in figure 22, where we can appreciate how for energies below the mentioned band all light that impinges on the sample travels in a straight line and produces a bright spot in the centre of the diffraction pattern. However, for energies above the edge of that band (1.07 in a/λ units) the onset of diffraction is evidenced by the spots in hexagonal arrangement revealing the symmetry of the crystal.

In summary, this merely highlights the fact that all optical phenomena occurring in PCs can be regarded as the interaction of light with the photonic states and accounted for in terms of PBG structure, and diffraction is only one example.

These scattering processes leading to phenomena of transmission, reflection and diffraction in general can be illustrated by analysing them in the *negligible contrast* approximation (nearly free electrons in solid state physics) where periodicity is assumed that brings a reciprocal lattice about while, contrast being so low, a homogeneous medium can still be assumed. In these circumstances energy and momentum conservation reduce to (i) incoming and outgoing wavevectors lying on the same circle ($\omega = c|\mathbf{k}|$) and (ii) their tips pointing to equivalent places in the repeated BZ tiling of the reciprocal space (differing by one reciprocal lattice vector: segments joining any two BZ centres). Therefore, the opening of the first pseudogap (L) is brought about by the build up of a stationary state as a result of incoming and outgoing wavevectors being opposite and their (equal) magnitude half

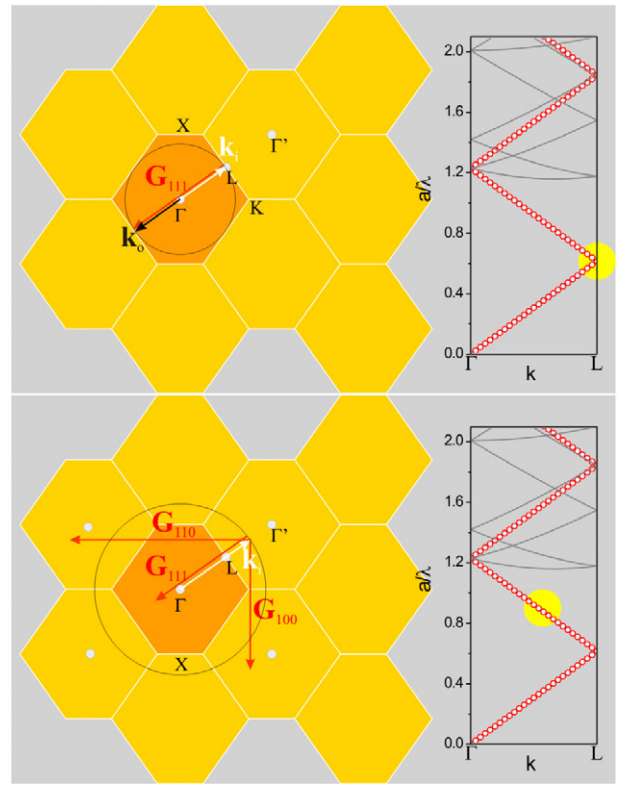


Figure 23. Those bands that fold back into the first BZ give rise to gaps in the centre and edge of the BZ when the Bragg condition is satisfied. In that case the incoming and outgoing wavevectors are opposite and equal in magnitude: they describe a process of reflection.

a reciprocal lattice vector. Thus the incoming field can couple to the outgoing one in a process of reflection and a Bragg peak forms in the spectrum. This is depicted in the upper panel of figure 23. If the energy is higher (lower panel in figure 23) or lower no outgoing wavevector can be found that complies with both conditions and the incoming field can only propagate forwards. This very argument can be extended to higher orders simply by enlarging the incoming, outgoing and reciprocal lattice vectors to account for higher gaps.

As was mentioned earlier, other bands in the PBG diagram (like the green band in figure 6) can be seen as originating from the dispersion relation for wavevectors lying on lines that can be translated by one reciprocal lattice vector to coincide with the line ΓL as analysed in the previous paragraph. Of course, since the line does pass through the origin the smallest energy can be readily appreciated to be greater than zero and given by this distance from the line to the origin. The wavevector at which this minimum occurs is perpendicular to the ΓL direction under consideration, meaning that, in general, this minimum can occur anywhere in the ΓL panel in the dispersion diagram of the PBG structure, not necessarily in the centre or edge because the folding reciprocal lattice vector needs not be perpendicular to ΓL . See figure 24, upper panel. Again along this line we can find points where energy and momentum are conserved, giving rise to scattering processes, and others where light can only propagate. This is shown in figure 24, where the lower panel illustrates the opening of the gap at the edge of the BZ while the upper panel shows a propagating state since no

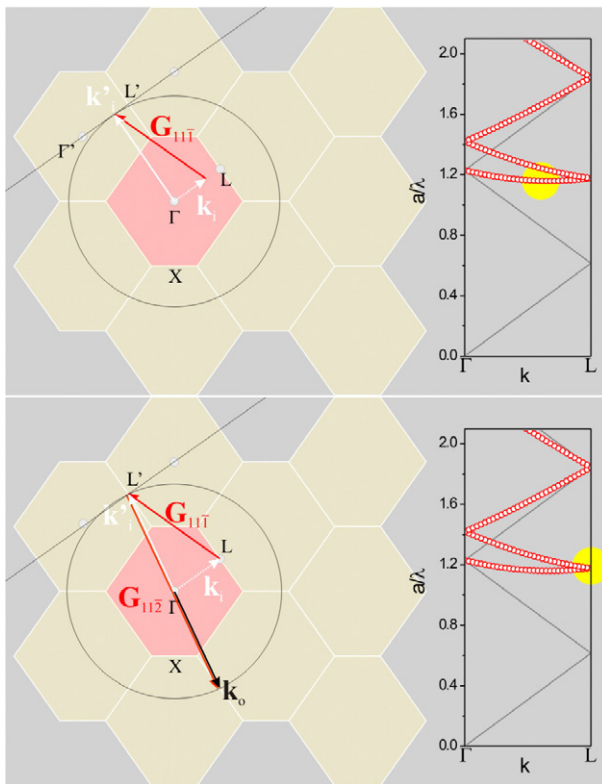


Figure 24. Bands originating from wavevectors that fold back into the first BZ through reciprocal lattice vectors ($\mathbf{G}_{(111)}$ in this case) non-collinear with the direction under analysis [111] give rise to bands that do not go to zero energy and have a minimum not in the origin. Gaps in the centre and edge of the BZ open when the Bragg condition is held. In this case the incoming and outgoing wavevectors need not be opposite, and correspond to a *diffraction*.

scattering processes are possible: no reciprocal lattice vector can map the tip of \mathbf{k}'_{in} into the circle. This analysis can be extended to all other directions possible in order to complete all the bands in an altogether similar procedure.

Some of the processes where scattering takes place open gaps in the edge while others open the gaps in the centre of the BZ. However, while a given scattering process may open a gap in the centre or edge, other bands and gaps can populate that energy range, compete for scattering strength, and share the intensity. For that reason reflectance peaks, for instance, will decrease in intensity as we scan higher and higher in energy. This means that the higher the energy the more widespread the scattered rays will be. It becomes clear that as we reach higher and higher in energy more processes are involved and the interpretation of the bands can hardly be done otherwise than numerically; however, the fundamental phenomenon is basically as simple as in the case of the Bragg peak. An analysis incorporating the magnitudes of the Fourier components of the states involved in the process of scattering and the magnitudes of the couplings may become useful in trying to fully understand all these phenomena.

To summarize, photonic band gap materials have shown to hold the key to many demands of the future photonics technology. In their understanding, most of the notions can be borrowed from solid state physics, which helps in explaining observed phenomena and in predicting new ones.

From the early days when the concept was first proposed numerous applications have been demonstrated and many fabrication techniques tested. Foremost among the approaches to PCs, colloidal systems lend themselves to be used as natural starting points for the purpose of creating and using photonic crystals and casting light on many facts. A broad range of techniques and different sources of knowledge contribute to the interdisciplinary nature of the subject as a host of materials properties are involved that spring from their architectural scale.

Acknowledgments

This work was partially supported by the Spanish CICyT project MAT2003-01237, the Comunidad Autónoma de Madrid under contract GR/MAT/0430/2004 and European Union Network of Excellence IST 511616: *PhOREMOST*. The author wishes to express his most sincere thanks to the members of the Photonic Crystals Group of ICMM for their support and for being the actual doers of all the work here reported only partially.

References

- [1] Hinton H E and Gibbs D F 1969 *J. Insect. Physiol.* **15** 959
- [2] Sanders J V 1964 *Nature* **204** 1151
- [3] Kittel C 1968 *Introduction to Solid State Physics* 3rd edn (New York: Wiley)
- [4] Tarhan İ İ and Watson G H 1996 *Phys. Rev. B* **54** 7593
- [5] Shung K W K and Tsai Y C 1993 *Phys. Rev. B* **48** 11265
- [6] Leung K M and Liu Y F 1990 *Phys. Rev. Lett.* **65** 2646
- [7] Zhang Z and Satpathy S 1990 *Phys. Rev. Lett.* **65** 2650
- [8] Ho K M, Chan C T and Soukoulis C M 1990 *Phys. Rev. Lett.* **65** 3152
- [9] Joannopoulos J D, Meade R D and Winn J N 1995 *Photonic Crystals: Molding the Flow of Light* (Princeton, NJ: Princeton University Press)
- [10] Sakoda K 2001 *Optical Properties of Photonic Crystals (Springer Series in Optical Sciences vol 80)* (Berlin: Springer)
- [11] Johnson S G and Joannopoulos J D 2001 *Opt. Express* **8** 173
- [12] Sözüer S, Haus J W and Inguva R 1993 *Phys. Rev. B* **45** 13962
- [13] Ashcroft N W and Mermin N D 1976 *Solid State Physics* (Philadelphia, PA: Rinehart and Wilson)
- [14] López C 2003 *Adv. Mater.* **15** 1680
- [15] Yablonovitch E, Gmitter T J and Leung K M 1991 *Phys. Rev. Lett.* **67** 2295
- [16] Lim K Y, Ripin D J, Petrich G S, Kolodziejski L A, Ippen E P, Mondol M, Smith H I, Villeneuve P R, Fan S and Joannopoulos J D 1991 *J. Vac. Sci. Technol. B* **17** 1171
- [17] Wendt J R, Vawter G A, Gourley P L, Brennan T M and Hammons B E 1993 *J. Vac. Sci. Technol. B* **11** 2637
- [18] Noda S, Chutinan A and Imada M 2000 *Nature* **407** 608
- [19] Lin S Y, Fleming J G, Hetherington D L, Smith B K, Biswas R, Ho K M, Sigalas M M, Zubrzycki W, Kurtz S R and Bur J 1998 *Nature* **394** 251
- [20] Noda S, Tomoda K, Yamamoto N and Chutinan A 2000 *Science* **289** 604
- [21] Qi M, Lidorikis E, Rakich P T, Johnson S G, Joannopoulos J D, Ippen E P and Smith H I 2004 *Nature* **429** 538
- [22] Campbell M, Sharp D N, Harrison M T, Denning R G and Turberfield A J 2000 *Nature* **404** 53
- [23] Lee W M, Pruzinsky S A and Braun P V 2002 *Adv. Mater.* **14** 271
- [24] Lai N D, Liang W P, Lina J H, Hsu C C and Linc C H 2005 *Opt. Express* **13** 9605
- [25] Sun H B, Matsuo S and Misawa H 1999 *Appl. Phys. Lett.* **74** 786

- [25] Seet K K, Mizeikis V, Matsuo S, Joudkazis S and Misawa H 2005 *Adv. Mater.* **17** 541
- [26] Robbie K and Brett M J 1997 *J. Vac. Sci. Technol. A* **15** 1460
- [27] Toader O and John S 2001 *Science* **292** 1133
- [28] Deubel M, von Freymann G, Wegener M, Pereira S, Busch K and Soukoulis C M 2004 *Nat. Mater.* **3** 444
- [29] García-Santamaría F, Miyazaki H T, Urquía A, Ibisate M, Belmonte M, Shinya N, Meseguer F and Lopez C 2002 *Adv. Mater.* **14** 1144
- [30] Aoki K, Miyazaki H T, Hirayama H, Inoshita K, Baba T, Sakoda K, Shinya N and Aoyagi Y 2003 *Nat. Mater.* **2** 117
- [31] Mayoral R, Requena J, Moya J S, López C, Cintas A, Míguez H, Meseguer F, Vázquez A, Holgado M and Blanco A 1997 *Adv. Mater.* **9** 257
- [32] Holgado M *et al* 1999 *Langmuir* **15** 4701
- [33] Gates B, Quin D and Xia Y 1999 *Adv. Mater.* **11** 466
- [34] Jiang P, Bertone J F, Hwang K S and Colvin V L 1999 *Chem. Mater.* **11** 2132
- [35] Wong S, Kitaev V and Ozin G 2003 *J. Am. Chem. Soc.* **125** 15589
- [36] Cong H and Cao W 2003 *Langmuir* **19** 8177
- [37] Jiang P 2004 *J. Am. Chem. Soc.* **126** 13778
- [38] Bertone J F, Jiang P, Hwang K S, Mittleman D M and Colvin V L 1999 *Phys. Rev. Lett.* **83** 300
- [39] Galisteo-López J F, Palacios-Lidón E, Castillo-Martínez E and López C 2003 *Phys. Rev. B* **68** 115109
- [40] Juárez B H, Ibisate M, Palacios J M and López C 2003 *Adv. Mater.* **15** 319
- [41] Blanco A *et al* 2000 *Nature* **45** 437
- [42] Míguez H *et al* 2001 *Adv. Mater.* **13** 1634
- [43] García-Santamaría F, Ibisate M, Rodríguez I, Meseguer F and López C 2003 *Adv. Mater.* **15** 788
- [44] Marlow F and Dong W 2003 *Chem. Phys. Chem.* **4** 549
- [45] García-Santamaría F, Salgueiriño-Maceira V, Lopez C and Liz-Marzán L M 2002 *Langmuir* **18** 4519
- [46] Xu X, Friedman G, Humfeld K D, Majetich S A and Asher S A 2002 *Chem. Mater.* **14** 1249
- [47] Yin Y and Xia Y 2002 *Adv. Mater.* **14** 605
- [48] Míguez H, Yang S M, Tétreault N and Ozin G A 2002 *Adv. Mater.* **14** 1805
- [49] Tétreault N, Míguez H, Yang S M, Kitaev V and Ozin G A 2003 *Adv. Mater.* **15** 1167
- [50] Jiang G N, Ostojic R, Narat D M, Mittleman V L and Colvin L 2001 *Adv. Mater.* **13** 389
- [51] Wostyn K, Zhao Y, Schaetzen G, Hellemans L, Matsuda N, Clays K and Persoons A 2003 *Langmuir* **19** 4465
- [52] Yablonovitch E 1987 *Phys. Rev. Lett.* **58** 2059
- [53] Kosaka H, Kawashima T, Tomita A, Notomi M, Tamamura T, Sato T and Kawakami S 1998 *Phys. Rev. B* **58** 10096
- [54] Luo C Y, Johnson S G and Joannopoulos J D 2002 *Appl. Phys. Lett.* **81** 2352
- [55] Notomi M, Yamada K, Shinya A, Takahashi J, Takahashi C and Yokohama I 2001 *Phys. Rev. Lett.* **87** 253902
- [56] Galisteo J F and López C 2003 *Phys. Rev. B* **68** 115109
- [57] van Driel H M and Vos W L 2000 *Phys. Rev. B* **62** 9872
- [58] Romanov S G, Maka T, Sotomayor Torres C M, Muller M, Zentel R, Cassagne D, Manzanares-Martinez J and Jouanin C 2002 *Phys. Rev. E* **63** 56603
- [59] Fudouzi H and Xia Y 2003 *Langmuir* **19** 9653
- [60] Arsenault A, Míguez H, Kitaev V, Manners I and Ozin G 2003 *Adv. Mater.* **15** 503
- [61] Fujita M, Takahashi S, Tanaka Y, Asano T and Noda S 2005 *Science* **308** 1296
- [62] Lodahl P, van Driel A F, Nikolaev I S, Irman A, Overgaag K, Vanmaekelbergh D and Vos W L 2005 *Nature* **430** 654
- [63] John S 1987 *Phys. Rev. Lett.* **58** 2486
- [64] Knight J C, Birks T A, Cregan R F, Russell P S and de Sandro J P 1998 *Electron. Lett.* **34** 1347
- [65] Painter O, Lee R K, Scherer A, Yariv A, O'Brien J D, Dapkus P D and Kim I 1999 *Science* **284** 1819
- [66] Park H G, Kim S H, Kwon S H, Ju Y G, Yang J K, Baek J H, Kim S B and Lee Y H 2004 *Science* **305** 1444
- [67] Galisteo J F and López C 2004 *Phys. Rev. B* **70** 035108
- [68] García-Santamaría F, Galisteo J F, Braun P L and López C 2005 *Phys. Rev. B* **71** 195112